Electronic structure of transition metal-doped XNiSn and XCoSb (X = Hf,Zr) phases in the vicinity of the band gap

2008 J. Phys.: Condens. Matter 20 255220

(http://iopscience.iop.org/0953-8984/20/25/255220)

J. Phys.: Condens. Matter **20** (2008) 255220 (7pp) doi:10.1088/0953-8984/20/25/255220

Electronic structure of transition metal-doped XNiSn and XCoSb (X = Hf, Zr) phases in the vicinity of the band gap

J W Simonson and S J Poon

Department of Physics, University of Virginia, Charlottesville, VA 22904-4714, USA

E-mail: jws9n@virginia.edu

Received 8 April 2008, in final form 2 May 2008
Published 21 May 2008
Online at stacks.iop.org/JPhysCM/20/255220

Abstract

Half-Heusler alloys of the compositions $X_{1-a}A_aNi_{1-b}B_bSn$ and $X_{1-a}A_aCo_{1-b}B_bSb$ (X = Hf, Zr) were synthesized with transition metals (A, B) substituted at the X and Ni/Co sites with the values of a and b between 0 and 0.15. Thermopower and electrical resistivity measurements from room temperature to 1100 K were performed to investigate resultant modifications to the electronic band structure in the vicinity of the band gap. As a result of these substitutions, thermopower was typically reduced across the entire temperature spectrum, in some cases changing sign. In the case of XNiSn-type alloys, electrical resistivity curves were indicative of semiconducting behavior, except in the case of samples in which Sb was introduced to the Sn site as a dopant. XCoSb-type alloys, however, were found to exhibit metallic resistivity behavior for all substitutions investigated. Hall effect measurements were performed to confirm the dominant carrier type and carrier concentration. The effects of transition metal substitution on the locations of a dopant band and the pinned Fermi level were discussed in the light of recent first-principles electronic structure calculations for half-Heusler alloys. For some of the semiconducting alloys, the band gaps that were determined from the high temperature region of the resistivity curves were found to be in closer agreement with those obtained from calculations than previously reported.

1. Introduction

The half-Heusler phase is of the form XYZ and is based on transition metals, where X and Y are such metals and Z is sp-valent, and each species sits on one of three interpenetrating fcc lattices—X and Z together forming a rock salt structure and X and Y forming a zinc-blende structure. In part due to this high degree of symmetry, certain compositions of these phases exhibit semiconducting properties, despite often being wholly composed of metallic atoms. As a result, half-Heusler phases have attracted some degree of attention as prospective high temperature thermoelectric materials [1, 2], heavy fermion systems [3], or half-metallic ferromagnets [4, 5], with recent calculations predicting T_C values much higher than room temperature [6].

The novel electrical and magnetic properties of the system have spurred a number of first-principles studies of the electronic structure of these alloys, with most of the work done from the late 1980s to 1990s. Early on, it was postulated that the peculiar properties of certain compositions of the half-Heusler phase were caused by an energy gap at the Fermi energy. The size of this gap was estimated by investigating the temperature dependence of the resistivity at high temperatures, resulting in 0.120 eV for TiNiSn, 0.186 eV for ZrNiSn, and 0.220 eV for HfNiSn [7]. By the mid-nineties, first-principles band structures and densities of state of this class of materials were calculated within the local density approximation (LDA), predicting an indirect gap of approximately 0.5 eV, in part the result of strong p–d hybridization in the ΓX direction [8]. By the turn of the century, quantitative information had been produced from band structures using FLAPW (full linearized augmented plane wave method) and LMTO-ASA (linearized muffin-tin orbitals-atomic sphere approximation) calculations. In ZrNiSn, it was found that the bands directly below the

gap were shown to be of strong Ni-d character, while those above were calculated to be of primarily Zr-d character [9]. Moreover, Sn-p levels were shown not to provide a large contribution to the density of states (DOS) in the vicinity of the band gap, indicating that doping that site would merely result in increasing or decreasing the valence electron count (VEC) without otherwise modifying the band structure near the Fermi level.

Interest in possible spintronics applications spurred band structure studies of half-Heusler compounds over the course of this decade. Tight bonding LMTO-ASA calculations have shown that in half-Heusler compositions with a gap at or near the Fermi level, gap formation results in part from d–d orbital repulsion between the transition metal X and Co/Ni and that in both XNiSn and XCoSb, neither Sn nor Sb has a major contribution in the vicinity of the gap [10]. In either case, below the gap lie four Sn/Sb s and p bands and five bands of predominantly Ni- or Co-d character. The nine bands are filled when the VEC is 18. A comprehensive review of *ab initio* calculations of the electronic structure and resultant magnetic properties of semiconducting and half-metallic half-Heusler alloys has recently been published [11].

Studies of the effects of dopants on the band structure of these phases have only emerged in the past few years. TB-LMTO-ASA calculations of TiCoSb and TiNiSn with 25% Mn introduced to the Ti site show the formation of a Mn band within the gap, above the predominantly Ni-d or Co-d states at the top of the valence band [12]. In both cases, the creation of this band pushes the Fermi energy higher, thereby reducing the size of the gap measured. In a similar vein, Co substitution onto the Ni site of ZrNiSn in quantities of 0.5%–10% was studied by another group [13]. In this case the dopant sub-level is observed only just above the valence band, and the Fermi energy is pulled down to that level, indicating that the semiconductor has become overcompensated. This overcompensation also results in a change of the majority carrier from electrons to holes and hence a flipping of the sign of the thermopower.

The thermopower, or Seebeck coefficient, and electrical resistivity are important parameters for optimizing the figure of merit, ZT, of a thermoelectric alloy. The magnitude of the thermopower is governed by the width and sharpness of the band gap. A sharp gap is beneficial for high thermopower. The intent of this experimental study is to examine systematically the effects of transition metal dopants V, Cr, Mn, Fe, Co, Ni, and Cu on the band gap structure, and therefore the thermopower and electrical resistivity, in both the $Hf_{0.75}Zr_{0.25}NiSn$ and the $Hf_{0.5}Zr_{0.5}CoSb$ systems. This study also represents a first attempt to explore the possibility of enhancing ZT through band structure modification in half-Heusler alloys. In this study, while the effects of introducing transition metal dopant bands in the vicinity of the band gap can be understood in terms of the roles of band structure and atomic dopant levels, the utilization of these dopants has not led to an increase of thermoelectric properties, and therefore ZT, due largely to significant reductions in thermopower caused by the introduction of these dopant levels into the band gap.

2. Experimental procedure

In this study, $Hf_{0.75}Zr_{0.25}NiSn$ was doped with V, Cr, Mn, Fe, Co, and Cu on the Ni site and Ce, V, Mn, Co, and Cu on the Hf/Zr site. The $Hf_{0.5}Zr_{0.5}CoSb$ system was doped with Mn and Ni on the Co site. Alloys were prepared in nominal compositions using high purity (greater than 99.9%) elemental solid pieces by arc melting under flowing argon. In Sb-rich compositions, an additional 5% Sb by weight was added to offset evaporation during melting. The addition of extra Sb in these materials has been shown to lead to near-stoichiometric half-Heusler phases [14]. To promote homogeneity, each ingot was flipped and remelted twice. Ingots were then cut into rectangular blocks of typical dimensions (2 mm × 2 mm × 10 mm) for measurement. The samples were cleaned in acetone for several minutes, wrapped in Ta foil, sealed in evacuated quartz ampoules, and annealed at 800 °C for seven to ten days to improve crystalline ordering. The crystal structure and phase purity of the annealed samples were confirmed by two-circle powder x-ray diffraction with Cu Kα radiation. Thermopower and electrical resistivity measurements were made simultaneously from room temperature to 1100 K over the course of three hours. Electrical resistivity was measured with silver contacts via the DC four point probe method, and thermopower was measured by employing the differential technique with chromel–alumel thermocouples attached by pressure contact, as described previously [15]. Each thermoelectric measurement was calculated from a linear best fit routine from at least 40 voltage and temperature differences. Hall effect measurements on selected samples were performed on a Quantum Design PPMS with five contacts, two for alternating current and three for voltage measurement. Carrier concentration was calculated from the slope of Hall resistivity versus magnetic field curves.

3. Results and discussion

3.1. Structure

X-ray diffraction scans were taken to verify that the relatively high percentages of transition metal dopants were indeed associated into the half-Heusler crystal structure. Figure 1 is an example of one such scan, in this case $(Hf_{0.75}Zr_{0.25})_{0.9}Mn_{0.1}NiSn$, which clearly shows only the nine peaks associated with the half-Heusler phase. Similar scans were made on V-, Cr-, Mn-, Fe-, Co-, and Cu-doped samples, each of which showed no second phase. Any changes in the lattice constant as a result of substitution were too small to be measured, which is not surprising considering the relatively constant metallic radii for the transitional metal series V, Cr, Mn, Fe, Co, Ni, Cu.

3.2. Electrical resistivity and band gap

The position of the Fermi energy relative to the bottom of the conduction band was calculated from high temperature electrical resistivity measurements to provide an indication of the extent of acceptor doping, as well as to suggest the location of partially-filled dopant bands that exist within the

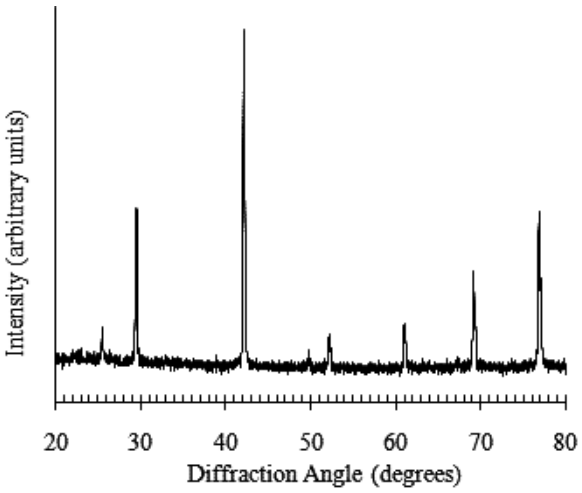

Figure 1. X-ray diffraction scan of $(Hf_{0.75}Zr_{0.25})_{0.9}Mn_{0.1}NiSn$, showing only the nine peaks associated with the half-Heusler phase.

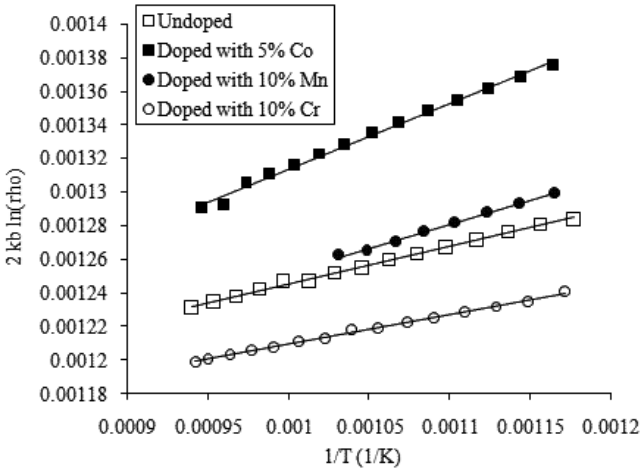

Figure 2. High temperature end of resistivity curves of $Hf_{0.75}Zr_{0.25}NiSn$ with transition metals doped to the Ni site, plotted to display linear relation between $1/T$ and $2k_B \ln \rho$.

Table 1. Effective gaps of doped $Hf_{0.75}Zr_{0.25}NiSn$ alloys.

Composition	Theoretical gap size (eV)	Effective gap size (eV)
ZrNiSn	0.50–0.51	
HfNiSn	0.48	
$Hf_{0.75}Zr_{0.25}NiSn$		0.23
$Hf_{0.75}Zr_{0.25}Co_{0.05}Ni_{0.95}Sn$		0.40
$(Hf_{0.75}Zr_{0.25})_{0.95}Co_{0.05}NiSn$		0.47
$Hf_{0.75}Zr_{0.25}Fe_{0.05}Ni_{0.95}Sn$		0.27
$Hf_{0.75}Zr_{0.25}Mn_{0.1}Ni_{0.9}Sn$		0.27
$(Hf_{0.75}Zr_{0.25})_{0.9}Mn_{0.1}NiSn$		0.27
$(Hf_{0.75}Zr_{0.25})_{0.9}Mn_{0.2}Ni_{0.9}Sn$		0.33
$Hf_{0.75}Zr_{0.25}Cr_{0.1}Ni_{0.9}Sn$		0.18
$Hf_{0.75}Zr_{0.25}V_{0.1}Ni_{0.9}Sn$		0.19
$Hf_{0.75}Zr_{0.25}Cu_{0.01}Ni_{0.99}Sn$		0.15
$(Hf_{0.75}Zr_{0.25})_{0.99}Cu_{0.01}NiSn$		0.12

band gap for these materials. Table 1 lists the position of the Fermi energy relative to the bottom of the conduction band—the so-called effective gap—of $Hf_{0.75}Zr_{0.25}NiSn$ with several transition metal dopants, calculated from high temperature electrical resistivity data using the method of Aliev *et al* [7] in which electrical resistivity is mainly determined by the effective gap size ε_g using the following relation:

$$\rho \sim \exp\left(\frac{\varepsilon_g}{2k_B T}\right).$$

For comparison, oft-cited theoretical values of the energy gaps of ZrNiSn [8, 16] and HfNiSn [8] are included as the first entries of the table. Since the Fermi energy is found to be located at the top of the valence band [9, 10, 17, 18], the two values should be similar in the case of a perfect single crystal. The difference between predicted and measured band gap values has been explained as stemming from site disorder that introduces a partially-filled nonzero DOS in the gap, which has been explained as a result of a lattice defect, possibly the interposition of Hf/Zr and Sn or excess Ni taking the form of a donor level [19].

Figure 2 is a plot of several high temperature resistivity curves, with $1/2k_B \ln \rho$ plotted against the inverse of the temperature, T; thus the effective energy gap is given by the slope of the lines. Temperatures of 800 K and greater were recently reported to be sufficiently high to study the intrinsic semiconductor region of XNiSn (X = Ti, Zr) [19]. The lines in figure 2 were fit by linear regression over the temperature range of approximately 800–1100 K. The fitted temperature range varied for some materials, particularly in cases where good electrical contacts could not be maintained at high temperatures; a notable case is that with 10% Mn doping, which is included in the figure. The most striking departure from the measured gap value of the undoped material is observed for the Co-substituted alloys. According to thermopower and Hall coefficient measurements, Co substitution also changes the room temperature majority carrier from electrons to holes. The Fermi level in this instance appears to have been lowered to nearly the top of the valence band, which is primarily of Ni-d character, resulting in a measured gap close to the theoretical value.

As different transition metal dopants are investigated, moving right to left across the periodic table, the Fermi energy appears to move from near the top of the valence band towards the predominantly Hf-/Zr-d conduction band edge, as is revealed by the measured gap size. The observed trend can be understood in terms of the energy level trend of the d states in the dopant elements [12]. Since the d electrons in the higher valent transition metals with larger nuclear charges, such as Co and Ni, are more tightly bound than those in the lower valent transition metals, such as V or Cr, the position of the impurity band of the p-type dopants Co, Fe, Mn, Cr, and V is expected to systematically shift inside the gap from lower energy to higher energy as the atomic number decreases. As a result, in the doped alloys with VEC less than 18, the Fermi level, which is now pinned at the partially-filled dopant impurity band, will systematically shift from lower energy to higher energy, starting from just above the filled Ni-d band, until the empty conduction band edge of predominantly Zr/Hf

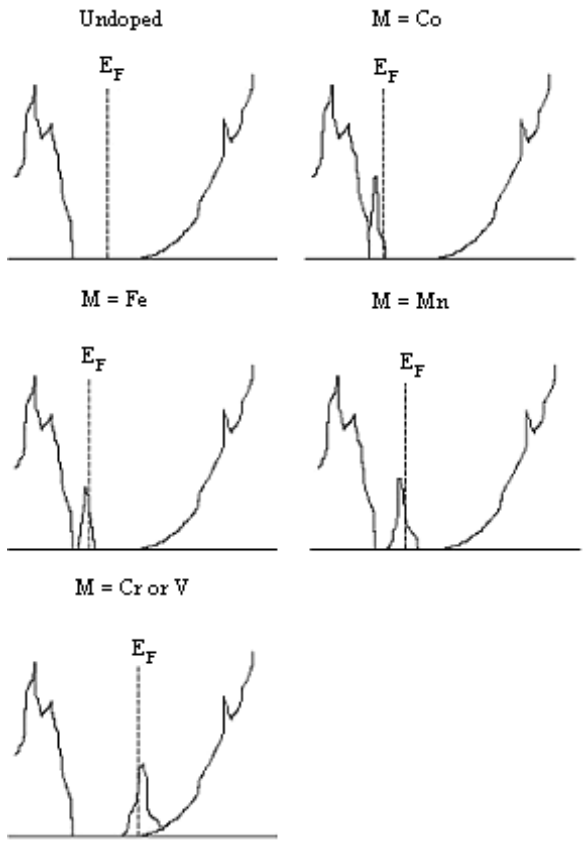

Figure 3. Sketch of band structure in the vicinity of the gap of XNiSn, showing the location of dopant peaks for different metals, M. The dopant bands are expected to be similar regardless of whether the dopant is introduced on the X site or the Ni site.

character is approached. To illustrate this point, a rough sketch of the band structure in the vicinity of the band gap is shown in figure 3. Overall, the dopant band location is largely determined by the atomic energy level of the dopant, and the effective gap size can be ascribed to the systematic variation of the dopant impurity band location inside the band gap with respect to the conduction band.

Dopants on the Hf/Zr site appear to produce a similar effect with dopant levels of a particular species occupying approximately the same position within the gap as it would for substitution on the Ni site; the effective band gap of $(Hf_{0.75}Zr_{0.25})_{0.9}Mn_{0.1}NiSn$, i.e. with 10% Mn substitution on the Hf/Zr site, was calculated to be 0.27 eV, the same value calculated for 10% Mn substitution to the Ni site. Furthermore, when 5% Co is added to the Hf/Zr site to form $(Hf_{0.75}Zr_{0.25})_{0.95}Co_{0.05}NiSn$, the resulting effective gap is calculated to be 0.47 eV, slightly larger than the 0.40 eV obtained when the Co is added to the Ni site. The reason behind this slight increase in ε_g may be attributed to the fact that in the case of 5% Co substitution on the Hf/Zr site, some of the Co-d electrons must fill the vacant bonding states that lie further below the top of valence band, originally occupied by the replaced 5% Hf/Zr [13]. As a result, both the Co dopant band and the pinned Fermi level shift to a lower energy, and a correspondingly larger effective band gap is observed.

Investigations were also made into the effective Fermi level of undoped and of transition metal-doped XCoSb alloys. Using the same method as above, an effective energy gap of 0.12 eV is calculated from high temperature resistivity measurements of $Hf_{0.5}Zr_{0.5}CoSb$. Such a small effective gap is not altogether surprising; it was previously reported that while TiCoSb was semiconducting, ZrCoSb and HfCoSb were high resistivity, compensated semimetals [20]. With regard to doped alloys, fitting high temperature resistivity curves was not possible for $Hf_{0.5}Zr_{0.5}CoSb$ alloys with Ni or Mn substituted onto the Co site or Sn substituted to the Sb site. All samples measured exhibited metallic resistivities, which increased with temperature, indicating that the Fermi level was no longer pinned within the gap.

3.3. Thermopower and hall effect measurements

A well-ordered system with a steep slope in the density of states near the Fermi level is favorable to large thermopower. Accordingly, any additional states that form in the vicinity of the band gap as a result of transition metal doping would tend to have a negative impact on the magnitude of the thermopower. The introduction of hole states in some of the alloys also tends to contribute to this reduction in the n-type host alloy. Table 2 is a table of room temperature values of thermopower, resistivity, and Hall measurements of the XNiSn-type half-Heusler compounds with transition metal substitutions, taken at approximately 310 K. It is noteworthy that when compared to the undoped XNiSn alloy, substitution with any transition metal located between Ni and Ti on the periodic table substantially reduces the thermopower without a very significant change in the resistivity, considering the relatively large change in valence. The dopant impurity bands pin the Fermi energy within the gap (figure 3), which results in high resistivity. Another factor that can also contribute to the higher resistivity in the case of d-band dopants, when compared with the much lower resistivity seen with sp-band dopants [2, 14] is that the d carriers are less mobile. Thus, transition metals are ineffective dopants for the half-Heusler alloys. The thermopower and resistivity trends can be discussed qualitatively. In the Co case, the partially unfilled Co dopant band overlaps with the valence band, introducing hole carriers into the system. As the Co concentration increases, the thermopower becomes more positive, and the additional hole carriers introduced into the system begin to lower the resistivity. The Fe dopant band has less overlap with the valence band, and there is less hole contribution to the thermopower. For the Mn-substituted alloy, the thermopower is less affected, possibly because the Mn dopant band is further from either band edge [12, 13]. Following the discussion in section 3.2, the Cr and V dopant bands are expected to overlap with the conduction band, and as a result the Cr-and V-doped alloys behave like an n-doped material with a reduced resistivity and thermopower [15].

Room temperature Hall measurements were carried out to determine carrier types and concentrations in selected samples, including undoped $Hf_{0.75}Zr_{0.25}NiSn$, and several doped $Hf_{0.75}Zr_{0.25}NiSn$ alloys, as shown in table 2. In both

Table 2. Room temperature thermopower, resistivity and Hall measurements.

Composition	Thermopower (μV K^{-1})	Resistivity ($\mu\Omega$ cm)	Carrier type	Carrier concentration (cm^{-3})
$Hf_{0.75}Zr_{0.25}NiSn$	−213	6800	Electrons	5.5×10^{19}
$Hf_{0.75}Zr_{0.25}Ni_{0.99}Cu_{0.01}Sn$	−71	1700	Electrons	2.2×10^{20}
$(Hf_{0.75}Zr_{0.25})_{0.99}Cu_{0.01}NiSn$	−171	1480		
$Hf_{0.75}Zr_{0.25}Co_{0.05}Ni_{0.95}Sn$	36	6700	Holes	3.1×10^{20}
$Hf_{0.75}Zr_{0.25}Co_{0.15}Ni_{0.85}Sn$	56	3800	Holes	7.3×10^{20}
$(Hf_{0.75}Zr_{0.25})_{0.97}Co_{0.18}Ni_{0.85}Sn$	25	4420		
$Hf_{0.75}Zr_{0.25}Fe_{0.05}Ni_{0.95}Sn$	−86	6750	Electrons	Obscured by magnetic effects
$Hf_{0.75}Zr_{0.25}Mn_{0.1}Ni_{0.9}Sn$	−172	7050	Electrons	5.4×10^{19}
$(Hf_{0.75}Zr_{0.25})_{0.9}Mn_{0.1}NiSn$	−201	8000	Electrons	4.1×10^{19}
$(Hf_{0.75}Zr_{0.25})_{0.9}Mn_{0.2}Ni_{0.9}Sn$	−195	4000		
$Hf_{0.75}Zr_{0.25}Cr_{0.1}Ni_{0.9}Sn$	−100	2645		
$Hf_{0.75}Zr_{0.25}V_{0.1}Ni_{0.9}Sn$	−129	2370	Electrons	2.6×10^{20}
$(Hf_{0.75}Zr_{0.25})_{0.9}V_{0.1}NiSn$	−161	4900		
$(Hf_{0.75}Zr_{0.25})_{0.9}Ce_{0.1}NiSn$	−36	2300		

samples doped with Co, holes were found to be the dominant carrier at room temperature, in agreement with the sign of the thermopower for those materials, as reported in the table. The carrier concentration of the sample with 15% Co was measured to be 7.3×10^{20} cm^{-3}, just under two-and-a-half times the measured value of the sample with 5% Co, 3.1×10^{20} cm^{-3}. This measurement is in qualitative agreement with the measured values of the electrical resistivity of those samples at room temperature. Hall measurements of the Mn-doped and V-doped samples also show good correlation with electrical resistivity measurements, and in each case the correct dominant carrier type is confirmed; the majority carrier in each of these materials was determined to be electrons, corresponding with the negative thermopower measurements. The carrier concentration for Mn doped to the Ni site was slightly higher than that of the sample with Mn doped to the Hf/Zr site: 5.4×10^{19} and 4.1×10^{19} cm^{-3}, respectively. This result is in agreement with the slightly higher resistivity for the sample with Mn doped to the Hf/Zr site, while the higher carrier concentration of the V-doped alloy corresponds with that material's lower resistivity. Plots of resistivity versus magnetic field for the Fe-doped composition were not found to be linear, preventing the calculation of carrier concentration for that alloy; the nonlinearity is assumed to be the product of a magnetic effect.

In comparison, Cu appears to be a more efficient dopant than the other transition metals studied. In stark contrast to other transition metal dopants, which have unfilled 3d shells, even a 1% substitution of Cu to the Ni site leads to an appreciably lower resistivity. It is speculated that, like in pure Cu, the s electrons in the Cu dopant atoms must reside in energy states above the filled d states. As a result, the Cu dopant band is expected to extend deep into the band gap, conceivably close to or even overlapping with the conduction band. Despite the greatly reduced resistivity at room temperature, the Cu-doped sample still exhibits a moderate decrease of resistivity with increasing temperature over the range 300–1100 K. This weak semiconducting behavior may be attributed to s–d hybridization, as part of the s dopant band is overlapped with the alloy's valence band. Figure 4 provides a comparison of resistivity measurements of $Hf_{0.75}Zr_{0.25}NiSn$ with 1% Cu doped to the Ni site and another sample with 1% Sb doped to the Sn site. Sb is an sp-band element and is known to be an effective dopant in half-Heusler alloys [15]; a previous study of doped MNiSn alloys performed by another group [21] reports a carrier concentration of 2.10×10^{20} cm^{-3} for the $Hf_{0.5}Zr_{0.5}NiSn_{0.99}Sb_{0.01}$ composition, within experimental error of the value measured for $Hf_{0.75}Zr_{0.25}Ni_{0.99}Cu_{0.01}Sn$ that is shown in table 2. As can be seen in the figure, however, even though both Cu and Sb add roughly an equal number of additional carriers to the system, the temperature dependence of the resistivity of the Cu-doped material remains semiconducting.

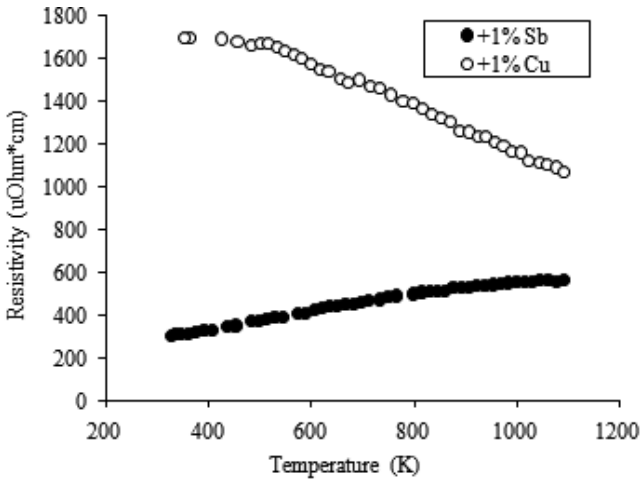

Figure 4. High temperature resistivity curves of $Hf_{0.75}Zr_{0.25}NiSn$ doped with 1% Sb to the Sn site and 1% Cu to the Ni site, demonstrating the likelihood of the Cu band entering the gap region.

Figure 5 is an overlay of several thermopower plots of transition metal-doped $Hf_{0.75}Zr_{0.25}NiSn$ over the same temperature region with the dopants on the Ni site. For all samples with transition metal dopants, the magnitude of the thermopower was measured to be lower than in the undoped case for the range of temperatures 300–1100 K, indicating that the transition metal dopant band within the gap is only partially filled, introducing more p-type carriers. The high temperature

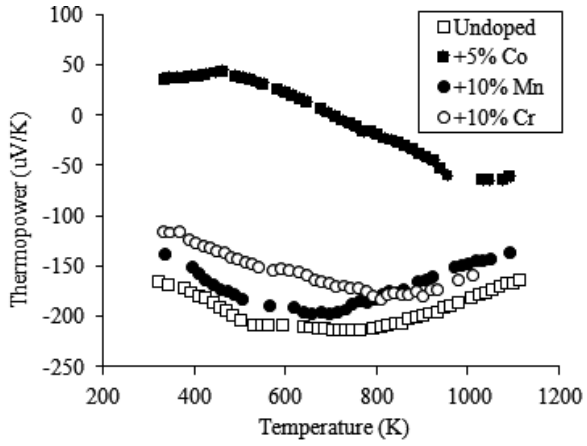

Figure 5. High temperature thermopower plots of several $Hf_{0.75}Zr_{0.25}NiSn$ materials doped with transition metals on the Ni site, showing lowering of thermopower and, in the case of Co substitution, over compensation.

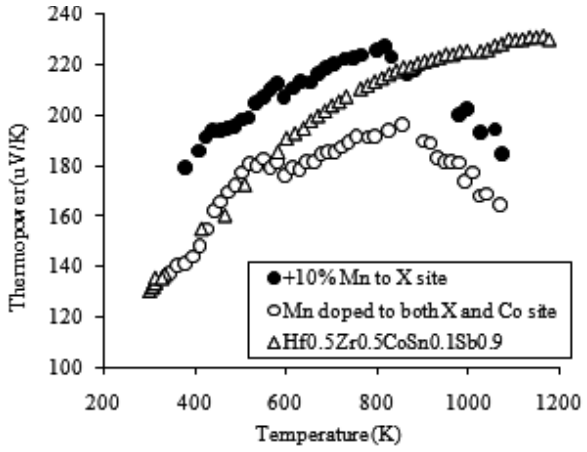

Figure 6. High temperature thermopower plots showing the effects of doping $(Hf_{0.5}Zr_{0.5})_{0.9}Mn_{0.25}Co_{0.85}Sn_{0.1}Sb_{0.9}$ and $(Hf_{0.5}Zr_{0.5})_{0.9}Mn_{0.1}CoSn_{0.1}Sb_{0.9}$.

rollover exhibited by most samples is caused by the further increase in hole carriers in the valence band as more electrons are promoted to the conduction band. The Co-substituted sample is a noteworthy standout; at room temperature, p-type conduction dominates until enough electrons have been promoted to the conduction band, causing the thermopower to change sign. This compensation occurs near 500 K for 5% Co substitution and 700 K for 15%.

$Hf_{0.5}Zr_{0.5}CoSb$ is an n-type thermoelectric material, but it is well known that a small amount of Sn doping to the Sb site drastically lowers the resistivity of the material while producing high p-type thermopower values [20]. The n-type to p-type thermopower transition occurs for Sn concentrations as low as 1%. Figure 6 is an overlay of thermopower measurements of $Hf_{0.5}Zr_{0.5}CoSn_{0.1}Sb_{0.9}$, $(Hf_{0.5}Zr_{0.5})_{0.9}Mn_{0.25}Co_{0.85}Sn_{0.1}Sb_{0.9}$, and $(Hf_{0.5}Zr_{0.5})_{0.9}Mn_{0.1}CoSn_{0.1}$–$Sb_{0.9}$, showing the effects of Mn doping on one and two sites of $Hf_{0.5}Zr_{0.5}CoSn_{0.1}Sb_{0.9}$. In terms of thermopower, the most marked result of adding Mn to this material is a high temperature rollover, likely caused by

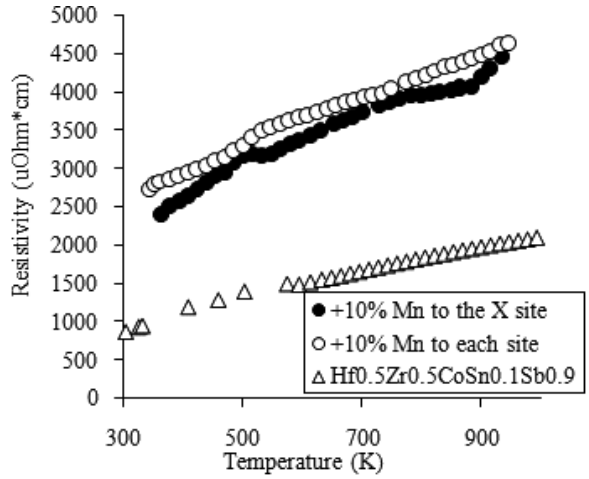

Figure 7. High temperature resistivity plots showing the effects of doping $(Hf_{0.5}Zr_{0.5})_{0.9}Mn_{0.25}Co_{0.85}Sn_{0.1}Sb_{0.9}$ and $(Hf_{0.5}Zr_{0.5})_{0.9}Mn_{0.1}CoSn_{0.1}Sb_{0.9}$.

the addition of extra p-type carriers to the system. At lower temperatures, however, the thermopower is about the same or even slightly improved by Mn doping, possibly due to the fact that the addition of a Mn band within the gap has little effect on the band edge of the material in such a wide gap compound (a gap of 0.95 eV is reported for TiCoSb) [17]. This explanation stands to scrutiny of resistivity data, namely that the resistivity increases dramatically due the addition of a localized Mn band within the gap, indicating that there is little if any overlap of this dopant band with the edge of either band. Figure 7 is an overlay of resistivity plots of the same three materials: undoped and Mn-doped $Hf_{0.5}Zr_{0.5}CoSn_{0.1}Sb_{0.9}$, and indeed resistivity is markedly increased by the Mn substitution over the entire range of temperature. Hence any marginal gains in the low to intermediate temperature thermopower measurement as a result of Mn substitution are wholly offset by the high temperature thermopower rollover and the increase—greater than a factor of two—in the electrical resistivity across the entire investigated range.

4. Conclusions

High temperature thermopower and electrical resistivity measurements of the $Hf_{0.75}Zr_{0.25}NiSn$ and $Hf_{0.5}Zr_{0.5}CoSn_{0.1}Sb_{0.9}$ half-Heusler phases were carried out to gain insight into the effects of transition metal dopants on the electronic structure in the vicinity of the band gap. Although, no increase in the thermoelectric figure of merit, ZT, was found, a good understanding of the effects of these dopants on electrical resistivity, thermal power, and Hall effect measurements has been reached. The results were discussed using band structure features obtained from recent first-principles electronic structure calculations of half-Heusler alloys. The measurements suggested that introduction of transition metal dopants resulted in the formation of dopant bands within the gap at positions dependent on the valance d-shell filling of the dopant atomic species. The resistivity and thermopower trends were found to be in agreement with those of the carrier concentration and mobility

obtained from Hall effect measurements. Effective energy gap calculations from high temperature resistivity measurements indicated the pinning of the Fermi level at the dopant bands. As a result, the band gaps obtained for some of the doped alloys were found to be in much closer agreement with theoretical values than previously reported. Finally, since the d electrons or holes in the transition metal dopant bands are localized within the band gap, they do not contribute to any significant reduction of electrical resistivity, but only to the suppression of thermopower. The exception to these findings is Cu doping on either transition metal site of XNiSn, which does not introduce localized states into the gap. Cu doping, however, does not lower the electrical resistivity as efficiently as does doping the Sn site with Sb. Consequently, the present d-band dopants have not led to improvement in the thermoelectric properties.

Acknowledgments

The authors wish to thank Dr Jiwei Lu and Dr Stuart Wolf of the Department of Material Science and Engineering at the University of Virginia for assistance with the Hall measurements.

References

[1] Poon S J 2001 *Recent Trends in Thermoelectric Materials Research I, Semiconductors and Semimetals* vol 70 (New York: Academic) p 37
[2] Nolas G S, Poon S J and Kanatzidis M 2006 *MRS Bull.* **30** 199
[3] Oppeneer P M, Antonov V N, Yaresco A N, Perlov A Y and Eschrig H 1997 *Phys. Rev. Lett.* **78** 4079
[4] Sanyal B, Eriksson O, Suresh K G, Dasgupta I, Nigam A K and Nordblad P 2006 *Appl. Phys. Lett.* **89** 212502
[5] Orgassa D, Fujiwara H, Schulthess T C and Butler W H 1999 *Phys. Rev.* B **60** 13237
[6] Dinh V A, Sato K and Katayama-Yoshida H 2008 *J. Phys. Soc. Japan.* **77** 014705
[7] Aliev F G, Brandt N B, Moshchalkov V V, Kozyrkov V V, Skolozdra R V and Belogorokhov A I 1989 *Z. Phys.* B **75** 167
[8] Ogut S and Rabe K M 1995 *Phys. Rev.* B **51** 10443
[9] Mahanti S D, Larson P, Chung D Y, Sportouch S and Kanatzidis M G 1999 *Mater. Res. Soc. Symp. Proc.* **545** 23
[10] Nanda B R K and Dasgupta I 2003 *J. Phys.: Condens. Matter* **15** 7307
[11] Galanakis I and Mavropoulos P 2007 *J. Phys.: Condens. Matter* **19** 315213
[12] Nanda B R K and Dasgupta I 2005 *J. Phys.: Condens. Matter* **17** 5037
[13] Romaka V A, Shelyapina M G, Gorelenko Y K, Fruchart D, Stadnyk Y V, Romaka L P and Ckeurin V F 2006 *Semiconductors* **40** 655
[14] Xia Y, Ponnambalam V, Bhattacharya S, Pope A L, Poon S J and Tritt T M 2001 *J. Phys.: Condens. Matter* **13** 77
[15] Culp S R, Poon S J, Hickman N, Tritt T M and Blumm J 2006 *Appl. Phys. Lett.* **88** 042106
[16] Larson P, Mahanti S D, Sportouch S and Kanatzidis M G 1999 *Phys. Rev.* B **59** 15660
[17] Tobola J and Pierre J 2000 *J. Alloys Compounds* **296** 243
[18] Stopa T, Tobola J, Kaprzyk S, Hill E K and Fruchart D 2006 *J. Phys.: Condens. Matter* **18** 6379
[19] Muta H, Kanemitsu T, Kurosaki K and Yamanaka S 2006 *Proc. Int. Conf. on Thermoelectrics* vol 25 p 120
[20] Xia Y, Bhattacharya S, Ponnambalam V, Pope A L, Poon S J and Tritt T M 2000 *J. Appl. Phys.* **88** 1952
[21] Uher C, Yang J, Hu S, Morelli D T and Meisner G P 1999 *Phys. Rev.* B **59** 8615